First-principles study of the electronic and optical properties of the (Y, N)-codoped anatase TiO_2 photocatalyst*

Lin Yan-Ming(林彦明)[a], Jiang Zhen-Yi(姜振益)[a]†, Hu Xiao-Yun(胡晓云)[b]‡,
Zhang Xiao-Dong(张小东)[a], Fan Jun(樊 君)[c],
Miao Hui(苗 慧)[b], and Shang Yi-Bo(商毅博)[b]

[a] *Institute of Modern Physics, Northwest University, Xi'an* 710069, *China*
[b] *Department of Physics, Northwest University, Xi'an* 710069, *China*
[c] *School of Chemical Engineering, Northwest University, Xi'an* 710069, *China*

(Received 11 June 2011; revised manuscript received 14 September 2011)

First-principles plane-wave pseudopotential calculations are performed to study the geometrical structures, formation energies, and electronic and optical properties of Y-doped, N-doped, and (Y, N)-codoped TiO_2. The calculated results show that Y and N codoping leads to lattice distortion, easier separation of photogenerated electron–hole pairs and band gap narrowing. The optical absorption spectra indicate that an obvious red-shift occurs upon Y and N codoping, which enhances visible-light photocatalytic activity.

Keywords: TiO_2, codoping, visible-light photocatalyst, first-principles calculation

PACS: 31.15.E–, 68.55.ag, 71.20.–b **DOI:** 10.1088/1674-1056/21/3/033103

1. Introduction

Titanium dioxide (TiO_2) as a semiconductor with a wide band gap (3.2 eV for anatase structures[1]) has been widely studied for several decades because of its superior properties in photoconversion and photocatalysis. It is an excellent material for energy production and environmental applications due to its characteristics of high chemical stability, low cost and good oxidation attributes.[2–4] TiO_2 has proved to be one of the most promising photocatalysts that can be widely used in pollutant degradation[5] and hydrogen generation.[6] However, its wide band gap leads to a low photon utilization efficiency of sunlight because only the ultraviolet light ($\lambda < 400$ nm) has the energy to transmit the electron from the valence band to the conduction band.[7,8] Furthermore, the photogenerated electron–hole pairs recombine relatively easily. Both of these factors inhibit its applications as a photocatalyst. Therefore, the extension of the optical absorption in TiO_2-based materials to the visible-light region, in conjunction with a low photogenerated electron–hole recombination rate, is of great practical importance.

An effective approach to extending the TiO_2 optical absorption edge into the visible-light region and reducing the photogenerated electron–hole recombination rate is to dope the TiO_2 with transition metal or non-metal elements. Transition-metal element doping can effectively reduce the electron–hole recombination rate, which promotes photocatalytic efficiency and extends the optical response from the ultraviolet region to the visible-light region. For example, Dholam *et al.*[9] reported on hydrogen production by photocatalytic water splitting using a Cr- or Fe-doped TiO_2 composite thin film as the photocatalyst. Zhang *et al.*[10] investigated the crystal and electronic band structures of undoped and Fe-doped anatase TiO_2 using the first-principles calculation. Gao *et al.*[11] studied the magnetism and electronic structure of the Cr-doped rutile TiO_2 based on the

*Project supported by the National Natural Science Foundation of China (Grant Nos. 10647008, 50971099, and 21176199), the Research Fund for the Doctoral Program of Higher Education, China (Grant Nos. 20096101110017 and 20096101110013), the Key Project of the Natural Science Foundation of Shaanxi Province, China (Grant Nos. 2010JZ002 and 2011JM1001), and the Graduate Innovation Fund of Northwest University, China (Grant No. 10YZZ38).

†Corresponding author. E-mail: jiangzy@nwu.edu.cn
‡Corresponding author. E-mail: hxy3275@nwu.edu.cn

© 2012 Chinese Physical Society and IOP Publishing Ltd

first-principles calculation, and the electronic structure analysis indicated that the oxygen vacancy has a large effect on the electronic structure of the Cr-doped rutile TiO_2. Li *et al.*[12] studied the photocatalytic activity of nanoglued Sn-doped TiO_2, and the results suggested that an appropriate amount of Sn dopant can greatly increase the quantity of hydroxyl radicals generated by TiO_2 nanoparticles, which is responsible for the obvious increase in photocatalytic activity. Chiou and Juang[13] examined the photocatalytic degradation of phenol in aqueous solution by Pr-doped TiO_2 nanoparticles. The Pr-doped TiO_2 exhibits high activity for the photocatalytic degradation of phenol in the experiment, which is due to the presence of Pr ions in the TiO_2 nanoparticles, thus causing a significant absorption shift towards the visible-light region. For the non-metal element doping, the doping of N[14,15], C[16,17], Si,[18,19] and S[20] in TiO_2 can reduce its band gap and shift its optical absorption edge toward the visible-light region because the related impurity states are near the valence band edge, which can minimize their potential as recombination centers compared with transition-metal doping.[21] In addition, some scientists have attempted to improve the photocatalytics of TiO_2 by using the transition-metal and non-metal elements codoped method. Huang *et al.*[22] reported the aerosol-assisted flow synthesis of B-doped, Ni-doped and (B, Ni)-codoped TiO_2 solid and hollow microspheres for the photocatalytic removal of NO. Tan *et al.*[23] studied the visible-light absorption and the photocatalytic activity in (Mo, N)-codoped TiO_2. Long and English[24] studied the band gap engineering of (N, Ta)-codoped TiO_2 by using the first-principles calculation. Zhang *et al.*[25] investigated the electronic structure and the optical properties of anatase TiO_2 codoped with nitrogen and iron by using the first-principles calculation. These results suggest that TiO_2 materials codoped with transition-metal and non-metal elements can effectively extend their optical absorption edges from the ultraviolet region to the visible-light region and prevent the recombination of the electron–hole pairs.

Recently, (Y, N)-codoped TiO_2 photocatalysts have been synthesized by Zhang *et al.*[26] The results indicated that the doping of Y into TiO_2 can reduce the recombination of the electron–hole pairs, and the doping of N can enhance the photo-response in the visible-light region. Both effects are beneficial to improving the photocatalytic activity of (Y, N)-codoped TiO_2. However, the physical and chemical origins of the enhanced photocatalytic activity and optical absorption in the visible-light range remain unexplained. In the present work, the electronic and optical properties of (Y, N)-codoped anatase TiO_2 will be investigated using density functional theory (DFT) to reveal the microscopic mechanism of band gap narrowing and the origin of the enhanced photocatalytic activity. For comparison, the corresponding calculations and theoretical analyses are also conducted for pure, Y-doped and N-doped anatase TiO_2. Our theoretical analysis provides a probable explanation for the experimental work of Zhang *et al.*[26] We also discuss the thermodynamic properties of Y-doped, N-doped and (Y, N)-codoped TiO_2 by analyzing the calculated formation energies.

2. Computational details

We simulated yttrium and nitrogen codoping effects using a $2 \times 2 \times 1$ (48 atom) supercell of the unit bulk anatase TiO_2 (see Fig. 1). Varieties of possible doping models were considered, such as substitutional Y at the Ti site (Y@Ti), substitutional Y at the O site (Y@O), substitutional N at the Ti site (N@Ti), and substitutional N at the O site (N@O) for the bulk doped systems. For the codoped systems, Y was located either at the Ti or O site, and N was located at either the O or Ti site, i.e. Y@Ti and N@Ti, Y@O and N@O, Y@Ti and N@O, and Y@O and N@Ti. The optimized partial structures using the 48-atom $2 \times 2 \times 1$ supercell are shown in Fig. 2.

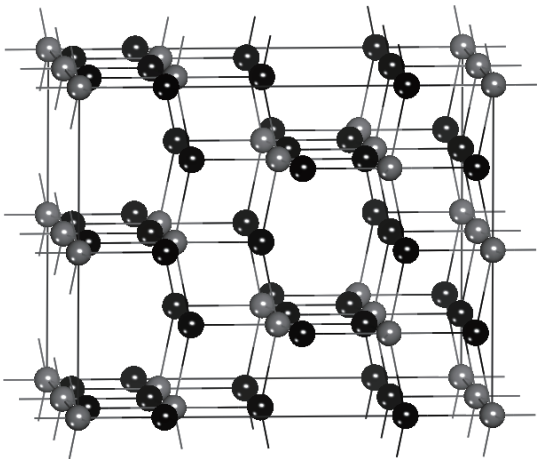


Fig. 1. The 48-atom anatase TiO_2 supercell. The gray spheres represent Ti atoms and the black spheres represent O atoms.

All the spin-polarized calculations were performed using the projector augmented wave (PAW) pseudopotential implemented in the VASP code.[27,28] The exchange–correlation potential was treated

by the generalized gradient approximation (GGA) with the Perdew–Wang parameterization (known as GGA-PW91).[29] The valence electron configurations, which included Ti ($3p^6 4s^2 3d^2$), O ($2s^2 2p^4$), Y ($4s^2 4p^6 5s^2 4d^1$), and N ($2s^2 2p^3$), were considered in this study. The wavefunctions were expanded with a kinetic energy cut-off of 400 eV, and the Monkhorst–Pack[30] grid parameter for k-point sampling was $5 \times 5 \times 5$. Geometry optimization and electronic structure calculations were carried out, and the block Davidson scheme was used for the geometry optimization. Cell and atomic relaxations were carried out until the residual force was below 0.01 eV/Å.

In the previous work, the electronic structure calculations were conducted using the GGA+U method[31] in conjunction with GGA geometry, which has led to a good description of TiO_2 based systems, such as Cr-doped TiO_2[11] and (N, Ta)-codoped TiO_2.[24] Therefore, all our electronic and optical property calculations for the Ti 3d and Y 4d electrons were conducted using the GGA+U method, which could produce good band gaps in comparison with the experimental results. It was found that the band gap of the pure anatase TiO_2 was 2.9 eV with $U = 10.0$ eV and $J = 1.0$ eV for the Ti 3d electrons, and only weakly dependent on J. This accords well with the experimental value of 3.2 eV.[1] For the Y-doped systems, the U and J values were 10.0 eV and 1.0 eV for the Y 4d electrons, respectively. As for the optical properties, the complex dielectric function $\xi = \xi_1 + \mathrm{i}\,\xi_2$, the real part ($\xi_1$), and the imaginary part (ξ_2) were calculated theoretically based on the DFT. The dielectric function can be defined in terms of current and field, which is most applicable for conductivity and optical responses. The corresponding absorption spectrum was estimated using the following equation:

$$I(\omega) = 2\omega \left(\frac{[\xi_1^2(\omega) + \xi_2^2(\omega)]^{1/2} - \xi_1(\omega)}{2} \right)^{1/2},$$

where I is the absorption coefficient, and ω is the angular frequency of the light.

3. Results and discussion

3.1. Geometry analysis

We performed structure optimization for the pure anatase TiO_2 supercell. The calculated lattice parameters of pure TiO_2 are $a = b = 3.816$ Å and $c = 9.618$ Å, which are in good agreement with the experimental values of $a = b = 3.782$ Å and $c = 9.502$ Å (within an error of 1.2%).[32] These results indicate that our calculation methods are reasonable, and the calculated results are authentic.

The average bond lengths of the doped TiO_2 obtained after the geometry optimization are listed in Table 1. For pure anatase TiO_2, the average Ti–O bond length is 1.977 Å, and there is no significant change compared with those of the Y- and N-doped ones. However, the average Ti–O bond length of the (Y, N)-codoped TiO_2 in the supercell is longer than those of the Y- and N-doped TiO_2. The average Y–O bond lengths in the Y-doped and (Y, N)-codoped systems are longer than the Ti–O bond length, as the radius of the Y ion is larger than that of the Ti ion. Due to the larger radius of the N atom, the average Ti–N bond lengths of the N-doped and the (Y, N)-codoped TiO_2 are also longer than those of the Ti–O bond. In the case of codoped TiO_2, the lengths of all these bonds are increased. The results show that (Y, N)-codoping leads to a significant lattice distortion and a high defect formation energy, which in turn changes the dipole and the moments, making the separation of the photo-excited electron–hole pairs easier.

Table 1. Average bond lengths (in units of Å) of doped TiO_2 after geometry optimization.

Bond	Pure TiO_2	Y-doped TiO_2	N-doped TiO_2	(Y, N)-codoped TiO_2
Ti–O	1.977	1.933	1.962	1.967
Ti–N	–	–	2.033	2.032
Y–O	–	2.128	–	2.130
Y–N	–	–	–	2.420

3.2. Defect formation energies

To probe the stabilities of the doped systems, we calculated the values of defect formation energy (E_f) for the doped and codoped systems according to the formulas

$$E_{\mathrm{f}(X@Y)} = E_{(X@Y)} - E_{(\mathrm{pure})} - (\mu_X - \mu_Y),$$

$$E_{\mathrm{f(Y@}Y\mathrm{and\ N@}Y)} = E_{\mathrm{(Y@}Y\mathrm{and\ N@}Y)} - E_{\mathrm{(pure)}} - (\mu_{\mathrm{Y}} + \mu_{\mathrm{N}} - \mu_Y - \mu_Y), \quad (X = \mathrm{Y}, \mathrm{N};\ Y = \mathrm{Ti}, \mathrm{O}),$$

where $E_{\mathrm{(pure)}}$ is the total energy of the host pure TiO_2 supercell, $E_{(X@Y)}$ and $E_{(\mathrm{Y@}Y\mathrm{and\ N@}Y)}$ are the total energies of the supercells containing the impurities. Under equilibrium conditions, the concentrations of point defects are controlled by their formation energies, which depend on the chemical potentials of the host and the impurity atoms. For TiO_2, the chemical potentials of O and Ti satisfy the relationships $\mu_{\mathrm{Ti}} + 2\mu_{\mathrm{O}} = \mu_{\mathrm{TiO_2}}, \mu_{\mathrm{O}} \leqslant \mu_{\mathrm{O_2}/2}$, and $\mu_{\mathrm{Ti}} \leqslant \mu_{\mathrm{Ti}}^{\mathrm{metal}}$. The chemical potential μ_{O} is determined by the energy of an O_2 molecule in the O-rich growth condition (corresponding to a high value of μ_{O}). The μ_{O} is the energy of an O atom in the O_2 molecule, μ_{Ti} is the energy of one Ti atom in the bulk Ti in the Ti-rich condition (corresponding to a high value of μ_{Ti}), μ_{Y} and μ_{N} are the chemical potentials of the Y and N impurities, which are calculated from the bulk Y and the N_2 molecules, respectively.

Our calculations give successful explanations of a variety of possible doped models, and the ion of the dopant may be dependent on the growth condition. It should be noted that the smaller the E_{f} value, the more easily the impurity ions can be incorporated into the TiO_2 supercell. Our calculated formation energies for all doped and codoped anatase TiO_2 are listed in Table 2. It can be observed that the formation energy of Y@Ti is lower than that of Y@O under both the Ti-rich and the O-rich growth conditions. It is shown that the Ti atom is easier to be replaced with the Y atom under both the Ti-rich and O-rich growth conditions. However, the formation energy of Y@O is slightly higher than that of Y@Ti under the Ti-rich growth condition. The partial geometry is shown in Fig. 2(a). For the N-doped TiO_2, our calculations suggest that the formation energy of N@O is much smaller than that of N@Ti under both the Ti-rich and O-rich growth conditions in the N-doped TiO_2, suggesting that the O atom is easier to be replaced with the N atom under both the Ti-rich and O-rich growth conditions. In particular, under the O-rich growth condition, the formation energy of N@O is negative, indicating that the N impurity is readily incorporated into the crystal. The corresponding partial geometry is shown in Fig. 2(b). Due to the fact that Y is located either at the Ti or O site, and N is located at either the O or Ti site in the codoped systems, the formation energy of the Y@Ti and N@O codoped system is much smaller than that of the other codoped systems under both the Ti-rich and O-rich growth conditions. These results indicate that the Y impurity prefers to substitute the Ti ion, and the N impurity prefers to substitute the O ion under both the Ti-rich and the O-rich growth conditions. Figure 2(c) shows the corresponding partial geometry.

Table 2. Defect formation energies of doped and codoped anatase TiO_2.

Doping	Defect formation energy/eV	
	Ti-rich	O-rich
Y@Ti	4.1313	0.8289
Y@O	4.7103	2.7876
N@Ti	16.1896	14.2669
N@O	0.1146	–3.1878
Y@Ti and N@Ti	11.0972	5.8721
Y@O and N@O	8.6646	3.4395
Y@Ti and N@O	4.3658	–0.8593
Y@O and N@Ti	13.0785	7.8534

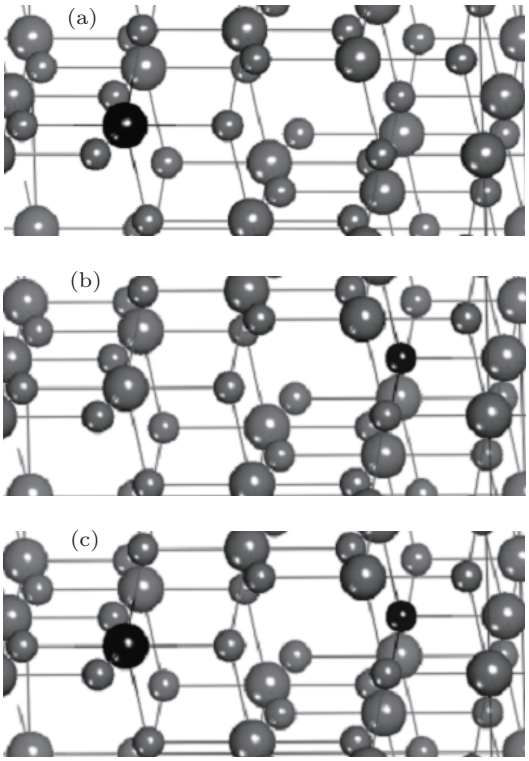


Fig. 2. Optimized partial structures using the 48-atom $2\times2\times1$ supercell for (a) Y-doped TiO_2, (b) N-doped TiO_2 and (c) (Y, N)-codoped TiO_2. The large gray spheres represent the Ti atoms, the small gray spheres represent the O atoms, the large black spheres represent the Y atoms and the small black spheres represent the N atoms.

3.3. Electronic properties

In order to analyse the electronic properties of the (co)doped anatase TiO_2, the total density of states

(TDOS) and the partial density of states (PDOS) were calculated using the GGA+U approach for both Ti 3d and Y 4d. The results are plotted in Fig. 3 for all the undoped and doped anatase TiO_2 with the up-spin DOS above zero and the down-spin DOS below zero. For pure TiO_2, the valence band (VB) is mainly contributed by the O 2p state, while the conduction band (CB) is mainly contributed by the Ti 3d state, as shown in Figs. 3(a) and 3(a′). The calculated band gap value is 2.9 eV, using the GGA+U scheme for the Ti 3d electrons, which accords well with the experimental value of 3.2 eV.[1] However, the calculated band gap value is 2.05 eV without the GGA+U scheme for the Ti 3d electrons. This result indicates that using the GGA+U scheme for the Ti 3d electrons can effectively reduce the underestimation of the energy gap by the GGA. For Y-doped (Y@Ti) TiO_2 (Figs. 3(b and b′)), we also use the GGA+U scheme for the Y 4d electrons in order to reduce the underestimation of the energy gap by the GGA. The shifts of the valence band maximum (VBM) and the conduction band minimum (CBM) are both about 0.2 eV upwards, and thus the band gap value is about 3.0 eV, which is due to the interaction between the Y 4d state and the Ti 3d state. Consequently, the electron transition energy from VB to CB increases about 0.1 eV compared with that of the pure anatase TiO_2, which improves the mobility of the photo-generated hole. Obviously, the higher the mobility of the photo-generated carriers (including holes and electrons), the better the performance of the photocatalysis. For the N-doped (N@O) TiO_2, it is clear from Figs. 3(c) and 3(c′) that an isolated N 2p state is localized just 0.5 eV above the top of the VB of the host TiO_2, which is because N is less electronegative than O. The electron in the VB can be excited to the localized impurity (N 2p) states in the forbidden gap and subsequently to the CB through visible-light absorption.

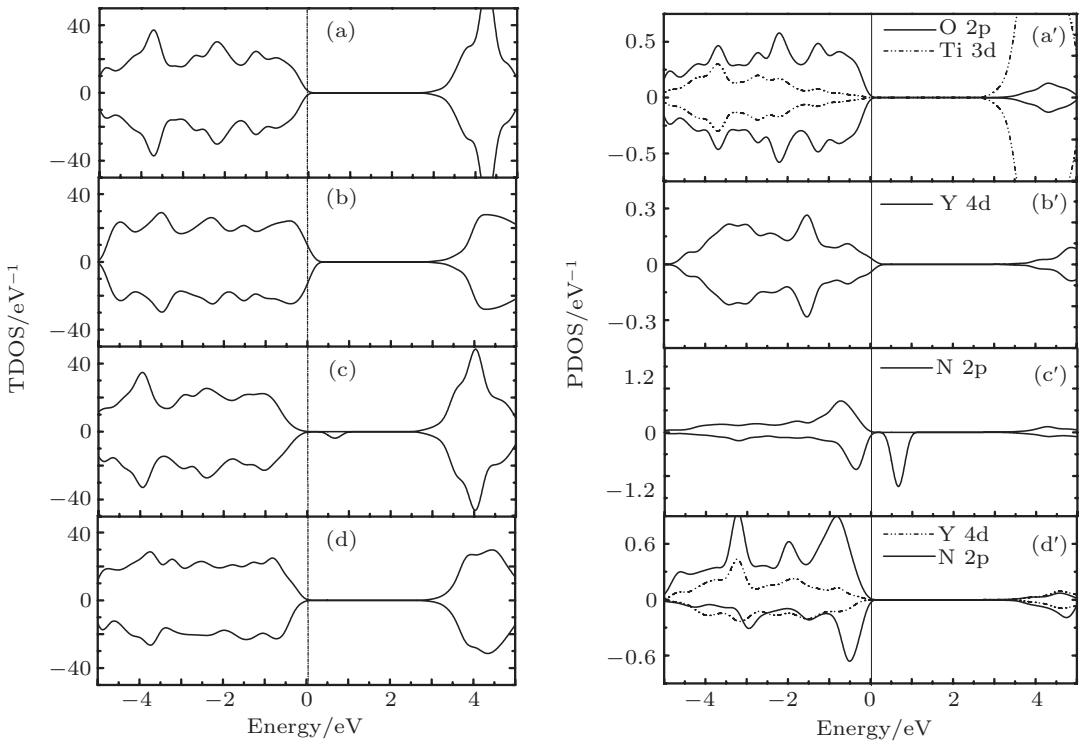


Fig. 3. Total densities of states (TDOSs) and partial densities of states (PDOSs) for ((a), (a′)) pure anatase TiO_2, ((b), (b′)) Y-doped TiO_2, ((c), (c′)) N-doped TiO_2 and ((d), (d′)) (Y, N)-codoped TiO_2. The top of the valence band of pure anatase is taken as the reference level.

For the (Y, N)-codoped (Y@Ti and N@O) anatase TiO_2, four different configurations, Y@Ti and N@Ti, Y@O and N@O, Y@Ti and N@O, and Y@O and N@Ti, were calculated according to the doping position. The results are shown in Figs. 3(d) and 3(d′). The calculations reveal that the defect formation energy of Y@Ti and N@O is the lowest. The valence band maximum has no obvious shift compared with that of the pure anatase, while the conduction band bottom has a significant decline (about 0.23 eV). Consequently, the electron transition energy from the VB to the CB has a decrease of about 0.23 eV, and

thus may induce a red-shift of the optical absorption edge. The calculated result gives a good explanation of the experimentally observed optical absorption broadening toward the longer wavelength in the (Y, N)-codoped TiO_2.

3.4. Optical properties

According to the obtained electronic structures, we calculated the optical absorption spectra of the pure and doped TiO_2 using the GGA+U method[31] for both the Ti 3d and Y 4d electrons, as show in Fig. 4. It is clear that the incorporation of N into the TiO_2 lattice induces the increase in the optical absorption in the visible-light region (about 590 nm), corresponding to a photo transition energy of 2.1 eV from the impurity states (N 3p) to the CB. However, the Y-doped TiO_2 system does not show any good absorption activity in the visible-light region. This is because the Y-doped TiO_2 has a broad band gap, leading to a low optical absorption, which is consistent with the experimental optical absorption spectra.[26]

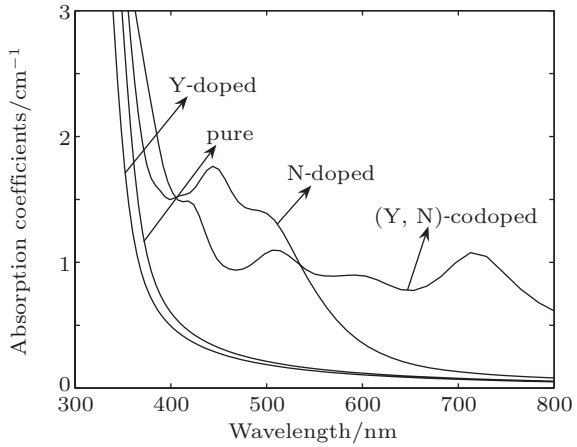


Fig. 4. Optical absorption spectra of pure and doped anatase TiO_2.

It is interesting that the absorption range in the (Y, N)-codoped TiO_2 system increases to 530 nm, and the absorption coefficient of the (Y, N)-codoping in the long wavelength range exceeds that of the N-doped TiO_2 due to the acceptor–donor impurity band in the band gap and the VB widening. In fact, the N-doped anatase TiO_2 compounds with various N-doping concentrations show different optical absorption spectra.[33] However, in the experiment, the growth of N-doped anatase TiO_2 becomes much more difficult when the N-doping level is increased.[34] Our theoretical studies find that the incorporation of Y into the N-doped TiO_2 can reduce the formation energy of N-doping, and thus increase the N-doping concentration, which can improve the absorption property of the anatase TiO_2.

4. Conclusion

We calculated the electronic and optical absorption properties of pure, Y-doped, N-doped and (Y, N)-codoped bulk anatase TiO_2 using spin-polarized density functional theory. The calculated results indicated that Y and N codoping leads to a lattice distortion, which changes the dipole moments and makes the separation of the photo-generated electron–hole pairs easier. Furthermore, Y and N codoping obviously induces band gap narrowing. The optical absorption spectra show that a significant red-shift occurs upon Y and N codoping, promoting the efficiency of the photocatalytic activity. The result suggests that (Y, N)-codoped TiO_2 is a highly active photocatalyst for efficient visible-light photocatalysis.

References

[1] Tang H, Lévy F, Berger H and Schmid P E 1995 *Phys. Rev.* B **52** 7771
[2] Tang J, Zou Z and Ye J 2004 *Catal. Lett.* **92** 53
[3] Hu L H, Dai S Y and Wang K J 2005 *Acta Phys. Sin.* **54** 1914 (in Chinese)
[4] Song G B, Liu F S, Peng T J, Liang J K and Rao G H 2002 *Acta Phys. Sin.* **51** 2793 (in Chinese)
[5] O'Regan B and Grätzel M 1991 *Nature* **353** 737
[6] Linsebigler A L, Lu G and Yates J T 1995 *Chem. Rev.* **95** 735
[7] Carp O, Huisman C L and Reller A 2004 *Solid State Chem.* **32** 33
[8] Fujishima A, Rao T N and Tryk D A 2000 *J. Photochem. Photobiol.* C **1** 1
[9] Dholam R, Patel N, Adami M and Miotello A 2009 *Int. J. Hydrogen Energy* **34** 5337
[10] Zhang X J, Gao P and Liu Q J 2010 *Acta Phys. Sin.* **59** 4930 (in Chinese)
[11] Gao G Y, Yao K L, Liu Z L, Zhang J, Li X L, Zhang J Q and Liu N 2007 *J. Magn. Magn. Mater.* **313** 210
[12] Li X, Xiong R and Wei G 2009 *J. Hazard. Mater.* **164** 587
[13] Chiou C and Juang R 2007 *J. Hazard. Mater.* **149** 1
[14] Asahi R, Morikawa T, Ohwaki T, Aoki K and Taga Y 2001 *Science* **293** 269
[15] Peng L P, Xu L and Yin J W 2007 *Acta Phys. Sin.* **56** 1585 (in Chinese)
[16] Park J H, Kim S and Bard A J 2006 *Nano Lett.* **6** 24
[17] Lettmann C, Hildenbrand K, Kisch H, Wacyk W and Maier W F 2001 *Appl. Catal.* B: *Environ.* **32** 215
[18] Jin R, Wu Z, Liu Y, Jiang B and Wang H 2009 *J. Hazard. Mater.* **161** 42

[19] Yang K, Dai Y and Huang B 2008 *Chem. Phys. Lett.* **456** 71

[20] Zhao Z Y, Liu Q J, Zhu Z Q and Zhang J 2008 *Acta Phys. Sin.* **57** 3760 (in Chinese)

[21] Wang H and Lewis J P 2006 *J. Phys.*: *Condens. Matter* **18** 421

[22] Huang Y, Ho W, Ai Z, Song X, Zhang L and Lee S 2009 *Appl. Catal.* B: *Environ.* **89** 398

[23] Tan K, Zhang H, Xie C, Zheng H, Gu Y and Zhang W F 2010 *Catal. Commun.* **11** 331

[24] Long R and English N J 2009 *Chem. Phys. Lett.* **478** 175

[25] Zhang Y, Tang C Q and Dai J 2005 *Acta Phys. Sin.* **54** 0323 (in Chinese)

[26] Zhang H, Tan K, Zheng H, Gu Y and Zhang W F 2011 *Mater. Chem. Phys.* **125** 156

[27] Kresse G and Hafner J 1994 *J. Phys. Rev.* B **47** 558

[28] Kresse G and Furthmüller J 1996 *J. Phys. Rev.* B **54** 11169

[29] Perdew J P, Chevary J A, Vosko S H, Jackson K A, Pederson M R, Singh D J and Fiolhais C 2004 *J. Phys. Rev.* B **46** 6671

[30] Monkhorst H J and Pack J D 1976 *Phys. Rev.* B **13** 5188

[31] Dudarev S L, Botton G A, Savrasov S Y, Humphreys C J and Sutton A P 1998 *J. Phys. Rev.* B **57** 1505

[32] Kuo M Y, Chen C L, Hua C Y, Yang H C and Shen P 2005 *J. Phys. Chem.* B **109** 8693

[33] Okato T, Sakano T and Obara M 2005 *Phys. Rev.* B **72** 115124

[34] Yang K, Dai Y and Huang B 2007 *J. Phys. Chem.* C **111** 12086